Received: 1 July 2022 | Revised: 8 November 2022 | Accepted: 27 December 2022

DOI: 10.1002/hed.27299

WILEY

ORIGINAL ARTICLE

The role of radiomics in tongue cancer: A new tool for prognosis prediction

Chiara Mossinelli MD[1] | **Marta Tagliabue MD**[1,2] | **Francesca Ruju MD**[3] | **Giulio Cammarata MSc**[4] | **Stefania Volpe MD**[5,6] | **Sara Raimondi PhD**[4] | **Mattia Zaffaroni MSc**[5] | **Johannes Lars Isaksson MSc**[5] | **Cristina Garibaldi MSc**[7] | **Marta Cremonesi MSc**[7] | **Federica Corso MSc**[4,8,9] | **Aurora Gaeta MSc**[4] | **Ilaria Emili MD**[3,10] | **Stefano Zorzi MD**[1] | **Daniela Alterio MD**[5] | **Giulia Marvaso MD**[5,6] | **Matteo Pepa MSc**[5] | **Elvio De Fiori MD**[3] | **Fausto Maffini MD**[11] | **Lorenzo Preda MD**[12,13] | **Marco Benazzo MD**[12,14] | **Barbara Alicja Jereczek-Fossa MD**[5,6] | **Mohssen Ansarin MD**[1]

[1]Department of Otorhinolaryngology and Head and Neck Surgery, European Institute of Oncology, IRCCS, Milan, Italy

[2]Department of Biomedical Sciences, University of Sassari, Sassari, Italy

[3]Division of Radiology, IEO, European Institute of Oncology, IRCCS, Milan, Italy

[4]Department of Experimental Oncology, IEO European Institute of Experimental Oncology IRCCS, Milan, Italy

[5]Division of Radiation Oncology, European Institute of Oncology, IRCCS, Milan, Italy

[6]Department of Oncology and Hemato-Oncology, University of Milan, Milan, Italy

[7]Unit of Radiation Research, IEO European Institute of Oncology, IRCCS, Milan, Italy

[8]Department of Mathematics (DMAT), Politecnico di Milano, Milan, Italy

[9]Centre for Health Data Science (CHDS), Human Techonopole

[10]ASST Centro Specialistico Ortopedico Traumatologico G. Pini/C.T.O, Milan, Italy

[11]Division of Pathology, IEO, European Institute of Oncology, IRCCS, Milan, Italy

[12]Department of Clinical, Surgical, Diagnostic, and Pediatric Sciences, University of Pavia, Pavia, Italy

[13]Division of Radiology, Fondazione IRCCS Policlinico San Matteo, Pavia, Italy

[14]Department of Otorhinolaryngology, Fondazione IRCCS Policlinico San Matteo, Pavia, Italy

Correspondence
Marta Tagliabue, Department of Otolaryngology and Head & Neck Surgery, European Institute of Oncology IRCCS, Via Ripamonti 435, 20141 Milano, Italy.
Email: marta.tagliabue@ieo.it

Stefania Volpe, Division of Radiation Oncology, European Institute of Oncology, IRCCS, Via Ripamonti 435, 20141 Milan, Italy.
Email: stefania.volpe@ieo.it

Abstract

Background: Radiomics represents an emerging field of precision-medicine. Its application in head and neck is still at the beginning.

Methods: Retrospective study about magnetic resonance imaging (MRI) based radiomics in oral tongue squamous cell carcinoma (OTSCC) surgically treated (2010–2019; 79 patients). All preoperative MRIs include different sequences (T1, T2, DWI, ADC). Tumor volume was manually segmented and exported to radiomic-software, to perform feature extraction. Statistically significant

Funding information
Italian Ministry of Health with Progetto di Eccellenza, Ricerca Corrente and 5x1000 funds

variables were included in multivariable analysis and related to survival endpoints. Predictive models were elaborated (clinical, radiomic, clinical-radiomic models) and compared using C-index.

Results: In almost all clinical-radiomic models radiomic-score maintained statistical significance. In all cases C-index was higher in clinical-radiomic models than in clinical ones. ADC provided the best fit to the models (C-index 0.98, 0.86, 0.84 in loco-regional recurrence, cause-specific mortality, overall survival, respectively).

Conclusion: MRI-based radiomics in OTSCC represents a promising noninvasive method of precision medicine, improving prognosis prediction before surgery.

KEYWORDS
mobile tongue cancer, oral cavity tumor, precision medicine, prognosis prediction, radiomics

1 | INTRODUCTION

The accurate prognosis prediction represents the first objective for tailored therapy selection in oncology. In particular, there are different available oncological therapies (surgery, radiotherapy, adrotherapy, chemotherapy, immunotherapy) and the prognosis prediction aim to intensify the therapeutic regimen in selected cases, especially in planning adjuvant treatment. In recent years, the scientific community has focused on finding accurate, repeatable, and noninvasive biomarkers to better stratify patients' prognosis, improve the effectiveness of treatments and reduce related side effects (therapeutic index). Moreover, the recent growing volume of data and the complexity of decision-making processes has contributed to the birth of the "precision medicine," that considers the variability of patients and diseases. An emerging field of precision medicine is represented by radiomics,[1] which consists in a high throughput extraction of quantitative features from conventional radiological imaging, with the aim of quantitatively describe the cancer "phenotype."[2,3] Radiomics permits to analyze tumor heterogeneity in a noninvasive, economical, and repeatable way, offering a potential tool for precision medicine in cancer treatment. The quantitative data extracted from radiomics are called "features" and can be referable both to the macroscopic disease and to the tumor microenvironment, providing distinct and complementary information to the clinical models. Thanks to its potential implications, in recent years radiomics has generated growing interest from the scientific community. A recent review reported that the annual growth rate in the number of radiomics articles published between 2013 and 2018 was 177.82%.[4] Most of the included works are mainly focused on breast, lung, and prostate cancer. Conversely, in head and neck cancer its development and application are still at the beginning, and available studies are limited and mostly focused on nasopharynx and oropharynx cancers.[5] Furthermore, the great prevalence of radiomics analysis is based on computed tomography, while application on magnetic resonance imaging (MRI) is more complex and less studied in head and neck disease.[6]

Despite the progress of the last few decades in diagnosis and treatment of oral tongue squamous cell carcinoma (OTSCC), the survival rates have improved in a marginal way. Nowadays the gold standard for OTSCC loco-regional staging is the MRI,[7,8] while the gold standard of treatment is represented by surgery.[9] In case of intermediate-advanced pathological stage (pT≥3, pN+) and/or presence of other negative prognostic factors (e.g. perineural infiltration) adjuvant radiotherapy is recommended.[9] In case of lymphnode metastases with extranodal extension (ENE), also adjuvant chemotherapy should be performed.[9] Immunotherapy is generally reserved in case of relapse (loco-regional or distant) refractory to platinum-based regimens and with tumor expression of PD-L1 combined positive score ≥1.[10]

Even with combined treatments, loco-regional relapses are frequent (40%) and the 5-year survival rate is still unsatisfactory (50%–60%).[11–16] The presence of metastases with extra nodal extension (ENE), positive surgical margins and higher depth of invasion (DOI) are considered as the most significant negative prognostic factors.[13,15,17–20] Another negative factor recently considered in literature is the quantitative lymphnode burden: Zumsteg et al.[21] showed that even in patients with ENE, positive margins or both, only those with metastases in more than six lymphnodes had improved survival with postoperative chemoradiation. In general, the research of specifical prognostic factors aims to predict unfavorable

outcomes in order to intensify therapeutic regimen in selected cases. In this regard radiomics could represent an added value in planning precision medicine.

In this study, we applied radiomics to preoperative MRI of patients with OTSCC, with the aim of defining potential prognostic biomarkers. We evaluated the association between radiomic features and oncological outcomes to preoperatively estimate the prognosis of these patients.

2 | MATERIALS AND METHODS

We performed a retrospective radiomic analysis on preoperative MRI of consecutive patients with OTSCC surgically treated at Istituto Europeo di Oncologia (IEO), Milano (Italy), between January 2010 and December 2019. The project was endorsed by Radiomic Board and Ethical Committee (ID-TRIAL 2520). All patients signed an informed consent for the anonymized use of data for clinical and scientific purposes.

2.1 | Inclusion criteria

- Age ≥18 years.
- Neoplasia of the mobile tongue.
- Histological diagnosis: squamous cell carcinoma.
- No previous head and neck treatment.
- Clinical and follow-up data availability.
- Availability of MRI DICOM (Digital Imaging and Communications in Medicine) including contrast enhanced T1-weighted (CE-T1) and T2-weighted (T2W) sequences, Diffusion Weighted Imaging (DWI), Apparent Diffusion Coefficient Map (ADC).
- MRI performed at IEO. All exams were acquired on AvantoFit 1.5Tesla scanner (Siemens Healthineers, Erlangen, Germany) with a 20-channel phased array coil dedicated to head and neck.

We collected the following data for each patient:

- Preoperative data: age, sex, smoking and alcohol habits, neoplasia subsite, radiological DOI, clinical TNM (7th–8th ed.).
- Preoperative MRI parameters: scanner type, matrix acquisition, slices' thickness and spacing, repetition time.
- MRI data. head and neck radiologists manually segmented the T tumor volume (region of interest, ROI) for each sequence of the three-dimensional MRI. The ROI were extracted by one single trainee radiologist under supervision by an expert radiologist (reducing the possible bias in ROI extraction by double check and consensus among the two radiologists). Cases were excluded if the primary tumor was not demonstrable or if images were significantly degraded by artifacts. ROI delineation on ADC map was performed on the b-900 images of the DWI acquisition. Images and ROI were extracted as radiotherapy (RT) Structure files on AW Server 3.2 workstation (GE Healthcare, Milwaukee, WI) and exported in DICOM to a radiomic software. Features extraction was performed using IBSI (Image Biomarker Standardization Initiative) compliant tool PyRadiomics v3.0.1 (Numpy version 1.20.3, SimpleITK version 2.0.2, PyWavelet version 1.1.1) with default settings.
- Surgical and histopathological data: time of surgery, type of glossectomy,[22] neck dissection, surgical reconstruction; histology and grading tumor, maximum diameter (mm) and histological DOI (mm) revised by pathologist; lymphnode micrometastases, multifocality, resection margins, lympho-vascular invasion, perineural infiltration, lymphnode metastases, ENE, T-N tract status (it consists in all the structures anatomically located between the primary tumor and the neck lymphnodes),[23] pathological TNM (7th–8th ed.). In particular, 8th ed. is reported only for descriptive and informative purpose. The therapeutic choice was done basing on 7th ed. for the majority of patients (study population treated between 2010 and 2019; 8th ed. published in 2017 and applied from 2018 onwards).
- Post-surgical data: adjuvant therapy; disease relapse (oral cavity, neck or distant metastases), last otorhinolaryngology evaluation, patients' status (updated in December 2020), cause and time of death.

For clinical variables, we performed a univariate analysis with cox regression models maintaining the oncological outcomes as endpoints (overall survival OS, locoregional recurrence LRR, cause specific mortality CSM). Patients' characteristics were summarized with descriptive statistics (frequency and percentages for categorical variables; median and Interquartile (IQR) range for continuous variables). Survival was calculated from the time of surgery to the date of death, recurrence, or last follow-up, whichever occurred first. Local recurrence includes relapses on T and/or N (distant metastases or second tumors were not included). Local recurrence was recorded as the time elapsed between the end of the treatment and the first appearance of disease.

All variables found to be statistically significant ($p < 0.10$) were included in the multivariable analysis (cox proportional hazard regression models) to assess their association as independent factors on survival endpoints. Risk estimates were quantified by hazard ratio

(HR) and 95% confidence intervals (CI). Radiomic information was aggregated in the statistical analysis in terms of "radiomic score." Feature selection was carried out by first removing highly correlated features (Spearman $\rho > 0.95$) and zero-variance features. The remaining features were grouped in clusters (iterative hierarchical clustering algorithm) which grouped features with Spearman correlation $\rho \geq 0.75$. From each cluster, the algorithm selected the feature mostly associated with each outcome (lowest univariate cox proportional hazard regression model *p*-value), removing the others. The task was iterated until no Spearman correlation $\rho \geq 0.75$ among features was found, to guarantee the redundant features exclusion from the following steps. Then a model-based approach was adopted, and standardized features were selected by a multivariable cox regression LASSO model performing a further feature selection. The parameter λ value was chosen using 5-folds cross validation as the parameter maximizing the C-index. After estimating the model, for each patient, the radiomic score was defined as the product between the regression coefficients and their respective feature values. We elaborated different predictive models for each survival endpoint: clinical model (pre- and post-treatment), radiomic model, clinical-radiomic model (pre- and post-treatment).

The models were compared using the C-index, a measure of goodness of fit for binary outcomes in a classification setting, which ranges from 0 (very poor predictive model) to 1 (hypothetical perfect predictive model). To assess the validity of the estimates, for each model, a Bootstrap analysis with 5000 repetitions was performed to determine a CI for the C-index estimate. A likelihood ratio test (LRT) was performed to assess whether the radiomic model introduction improved the clinical models performance. Lastly, a sensitivity analysis was performed to overcome possible overfitting concerns: for each clinical-radiomic model an in-sample 5-fold-cross-validation was implemented.

All analyses were repeated for CE-T1, T2W, DWI, ADC.

Analyses were performed using R(4.1.1) for Windows.

3 | RESULTS

Based on inclusion criteria, we retrospectively selected 79 patients (Figure 1); main descriptive results are reported in Table 1 and the complete set of data of all patients are reported in supplementary material (Table S1). Median age was 55 years (IQR 41–67), with a prevalence of males (59 men vs. 20 women) and smokers (62% vs. 38%). From a surgical point of view, the T-N tract was removed in 81% cases and resulted positive in 22% patients. Negative margins were achieved in 91% of cases. Lymphnodes occult metastases were present in 56% of the cohort. Patients' follow-up was update at December 2020: the median time of follow-up was 29 months (IQR 15.5–65 months).

The Kaplan–Meier estimates for 10-year LRR, CSM and OS are displayed in Figure 2. Figure 3 reported curves related to radiomic score in CE-T1 and ADC (T2W and DWI relative figures in Supplementary Material Figure S1). For each MRI sequence, the five statistical models below were estimated. Similar results were found for all sequences and complete results are reported in Supplementary Material (Tables S2–S4). In multivariable

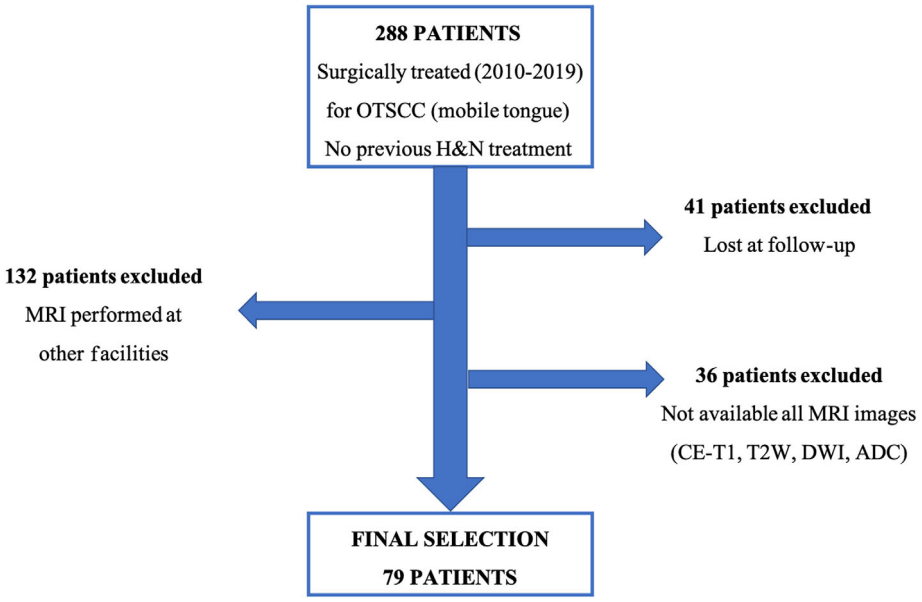

FIGURE 1 Flow diagram of patients' selection based on inclusion criteria. H&N, head and neck. [Color figure can be viewed at wileyonlinelibrary.com]

TABLE 1 Main characteristics of the study population: preoperative, surgical, histopathological, and follow-up data.

Characteristics		Median (IQR) or N (%)
Age		55 (41–67)
	≤45 years	24 (30%)
	>45 years	55 (70%)
Sex	Male	59 (75%)
	Female	20 (25%)
Smoking habits	No smoker	30 (38%)
	Ever smoker	49 (62%)
	Pack year[a]	30 (14.25–46.25)
cT (TNM VIII ed.)	cT1	3 (4%)
	cT2	25 (32%)
	cT3	48 (61%)
	cT4	3 (4%)
cN (TNM VIII ed.)	cN0	45 (57%)
	cN1	10 (13%)
	cN2	23 (29%)
	cN3	1 (1%)
Stage (TNM VIII ed.)	I	3 (4%)
	II	20 (25%)
	III	32 (41%)
	IV	24 (30%)
Grading	Not available	1 (1%)
	G1	18 (18%)
	G2	40 (51%)
	G3	20 (25%)
Tumor diameter (mm)		28 (20–42)
	≤20 mm	21 (27%)
	>20 mm and ≤ 40 mm	36 (45%)
	> 40 mm	22 (28%)
Histological DOI (mm)		11 (9.25–11)
	≤ 5 mm	12 (15%)
	> 5 mm and ≤10 mm	10 (13%)
	> 10 mm	57 (72%)
Surgical margins	Negative	72 (91%)
	Close (<1 mm)	4 (5%)
	Positive	3 (4%)
TN tract	Not removed	15 (19%)
	Negative	47 (59%)
	Positive	17 (22%)
pT (TNM VIII ed.)	pTis	1 (1%)
	pT1	10 (13%)
	pT2	10 (13%)
	pT3	35 (44%)
	pT4	23 (29%)
pN (TNM VIII ed.)	pNx	11 (14%)
	pN0	19 (24%)
	pN1	10 (12%)
	pN2	16 (21%)
	pN3	23 (29%)
Stage (TNM VIII ed.)	I	9 (11%)
	II	9 (11%)
	III	17 (22%)
	IV	44 (56%)
Adjuvant therapies	None	24 (30%)
	Radiotherapy	29 (37%)
	Chemoradiotherapy	26 (33%)
Follow-up	Time of follow-up (months)	29 (15.5–65)
	NED	55 (70%)
	AWD	24 (30%)
	Events timing (months)	8 (6–19)
	Dead for disease	23 (29%)
	Dead for other causes	9 (11%)

Note: Parameters are expressed in median and interquartile range (IQR) for continuous variables, number (*N*) and percentage for categorical variables. Events are classified in local relapse, regional relapse, distant metastases or second tumor. Events timing is defined as the time in months between the surgery and the event.

Abbreviations: AWD, alive with disease; DOI, depth of invasion; NED, not evidence of disease.

[a]Only for current smokers.

analysis, ADC provided the best fit to the models and related results are described in the text below. Tables 2–4 report results for LRR, CSM, and OS in ADC and also CE-T1 sequences, because it is the most widespread sequence (used in all MRI protocol in other facilities) and so it could be useful for external validation and future radiomics applications.

3.1 | Radiomic models

For LRR, CSM and OS, the feature selection algorithm yielded respectively 165, 170 and 174 features ($\rho < 0.75$). The radiomic score obtained after LASSO-cox regression

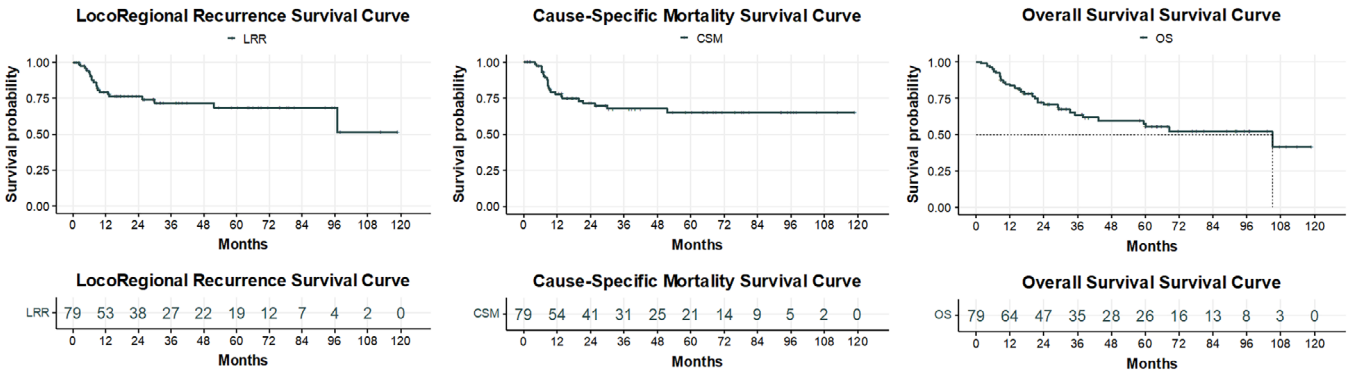

FIGURE 2 Kaplan–Meier estimates for 10 year loco-regional recurrence, cause specific mortality and overall survival. [Color figure can be viewed at wileyonlinelibrary.com]

model respectively included 33, 11 and 2 features. Features and radiomic score composition are reported in Supplementary Material. Radiomic score was significantly associated with each survival endpoint (HR 16.93, 5.28, 19.70 for LRR, CSM, OS, respectively; p-value <0.001 for all; Tables 2–4, Figure 1). Radiomic models provided an adequate fit for each endpoint, as shown by the C-index of 0.98 (95%CI [0.98, 1.00]) and 0.85 (95%CI [0.77, 0.91]) and 0.72 (95%CI [0.59, 0.78]) for LRR, CSM, and OS, respectively.

3.2 | Pre-treatment models

In the pre-treatment clinical model, for LRR, cN+ versus cN0 (7th ed.) resulted to be the only significant variable associated with a higher risk of recurrence (HR = 3.27, $p = 0.01$). Model's C-index was 0.68 (95%CI [0.48, 0.71]). After adding radiomic score (HR = 24.49, $p < 0.001$), in pre-treatment clinical-radiomic model, cN+ versus cN0 was no more significant and C-index significantly ($p < 0.001$) increased to 0.98 (95%CI [0.98, 1.00]).

For CSM, in the pre-treatment clinical model, only Stage III–IV versus I–II (7th ed.) was significantly associated with a worse outcome (HR = 3.85, $p = 0.03$). Model's C-index was 0.66 (95%CI [0.59, 0.80]). After adding radiomic score (HR = 6.00, $p < 0.001$), Stage III–IV was no more significantly and C-index significantly ($p < 0.001$) increased to 0.85 (95%CI [0.75, 0.90]).

Furthermore, OS was better for male compared to female sex (HR = 0.46, $p = 0.04$), slightly worse for older patients (HR = 1.02, $p = 0.09$) and for Stage III–IV (7th ed.) compared to Stage I–II (HR = 2.72, $p = 0.04$). Model's C-index was 0.70 (95%CI [0.57, 0.77]). In pre-treatment clinical-radiomic model, after adding radiomic score (HR = 22.17, $p < 0.001$), Stage III–IV was no more significant and the model's C-index significantly increased to 0.76 (95%CI [0.62, 0.78], p-value for the difference between clinical and clinical-radiomic model <0.001).

3.3 | Post-treatment models

For LRR, in the post-treatment clinical model, positive surgical margins (HR = 18.37, $p < 0.001$) and pN+ ECE + versus c/pN0 (HR = 14.51, $p < 0.001$) were significantly associated with a higher risk of recurrence. The model's C-index was 0.77 (95%CI [0.67, 0.85]). In the post-treatment clinical radiomic model, radiomic score (HR = 24.11, $p < 0.001$) was the only variable associated with the endpoint, with all the other variables becoming non-significant. After radiomic score was added, post-treatment clinical radiomic model C-index significantly ($p < 0.001$) increased to 0.98 (95%CI [0.98, 1.00]).

For CSM, in the post-treatment clinical model, male sex (HR = 0.36, $p = 0.03$), pN+ ECE− (HR = 12.33, $p = 0.002$), and pN+ ECE+ (HR = 12.87, $p < 0.001$) versus c/pN0 were significantly associated with the endpoint. The model's C-index was 0.77 (95%CI [0.70, 0.86]). In the post-treatment clinical-radiomic model, radiomic score (HR = 4.37, $p < 0.001$) and pN+ ECE+ versus c/pN0 (HR = 5.08, $p = 0.04$) were the only variables significantly associated with the endpoint. After radiomic score was added, post-treatment clinical radiomic model C-index significantly ($p < 0.001$) increased to 0.86 (95%CI [0.79, 0.91]). With T2W sequences, radiomic score was only borderline associated with CSM at multivariable analysis (HR = 7.86, $p = 0.06$, Supplementary Material Table S3) providing no significant increase in C-index after its inclusion in the model ($p = 0.06$).

A significantly better OS was observed for male patients (HR = 0.31, $p = 0.003$), while age at diagnosis and pathological status of lymphnodes pN+ ECE− and pN+ ECE+ versus c/pN0 were associated with a worse

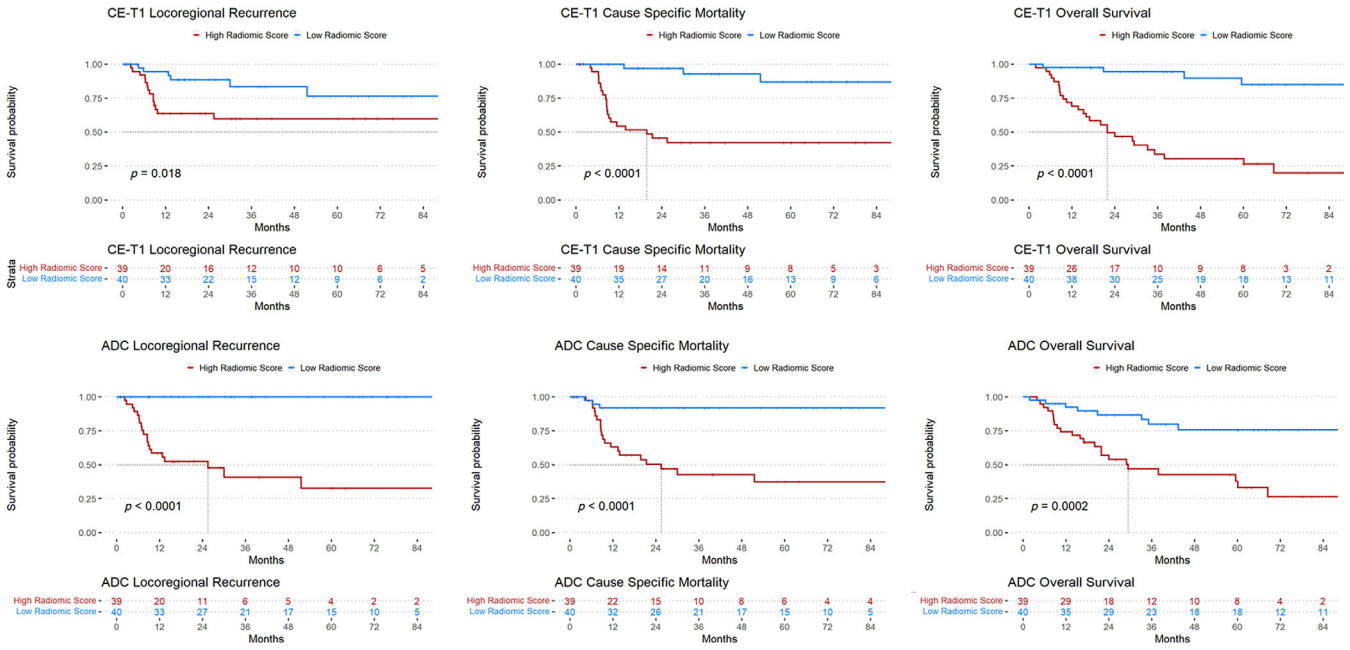

FIGURE 3 Kaplan–Meier plots for ADC (upper panels) and CE-T1 (lower panels) sequences according to high and low radiomic score, dichotomized based on its median value. Analogous curves relating to T2W and DWI are reported in Supplementary Material Figure S1. [Color figure can be viewed at wileyonlinelibrary.com]

OS (respectively HR = 1.03, $p = 0.02$ for age; HR = 7.28, $p = 0.002$ and HR = 14.78, $p < 0.001$ for the two categories of lymphnodes). The C-index of this model was 0.82 (95%CI [0.74, 0.86]). In the post-treatment clinical radiomic model, after adding radiomic score (HR = 7.72, $p = 0.005$), a reduction in pN+ ECE+ and pN+ ECE− versus c/pN0 HR was observed (HR = 4.58, $p = 0.03$ and HR = 10.21, $p < 0.001$, respectively), while C-index significantly ($p < 0.001$) increased to 0.84 (95%CI [0.79, 0.92]). Only with T2W sequences, radiomic score was borderline associated with OS at multivariable analysis (HR = 5.23, $p = 0.08$, Supplementary Material Table S4) providing no significant increase in C-index after its inclusion in the model ($p = 0.09$).

4 | DISCUSSION

In this study, we investigate whether radiomics could represent an added value to clinical variables in terms of prognosis (even predictive) in OTSCC. The protocol for proper MRI in this setting of patients includes T1- and T2-weighted sequences, CE-T1 with fat saturation and optionally DWI and ADC. The main advantage of DWI and ADC in the staging of OTSCC is the ability to distinguish between tumor and peritumoral inflammation.[24] We included all these sequences to access whether one sequence could fit better with radiomics and for all models the integration of radiomics with clinical variables improved the patients' outcome prediction. The highest value of C-index was found in ADC for LRR (0.98). Unfortunately, DWI sequences and ADC maps are optional and not performed in all radiological centers, limiting its potential application. There is a need to introduce DWI sequence and ADC map in standard protocol of MRI in OTSCC for its recognized added value in radiological staging.[24] Basing on our results, it could be also useful for prognosis prediction, opening the horizon for other radiomic studies. However, it must be taken into account that features can be influenced by the variety of scanning protocols and MRI-equipment, therefore MRI acquisition protocols needs to be standardized to try to validate radiomics models across different Facilities. Anyhow, our data showed excellent results also in CE-T1 sequences, which are commonly used, being easily available and interpretable. This allow radiomics to be applied to wider number of patients, regardless of the center where the MRI is performed.

The radiomic model related to data acquired in the preoperative phase. This information was retrieved before the surgery, unlike most other prognostic factors which are accessible only after pathological examination. The "pre-treatment information" represents a key point of precision medicine and tailored treatments.

In the pre-treatment clinical models, for OS, multivariate analysis confirmed that age, female sex and Stages III–IV, represent the main negative prognostic factors; adding the radiomic score to the model, the C-index was

TABLE 2 Loco-regional recurrence regression table for ADC and CE-T1 sequences.

	Pre-treatment model					Post-treatment model		
	Radiomic		Clinical	Clinical radiomic		Clinical	Clinical radiomic	
Sequence Variables	ADC HR [95%CI]	CE-T1 HR [95%CI]	HR [95%CI]	ADC HR [95%CI]	CE-T1 HR [95%CI]	HR [95%CI]	ADC HR [95%CI]	CE-T1 HR [95%CI]
Sex								
F	—	—	1	1	1	1	1	1
M	—	—	0.79 [0.30, 2.08]	2.88 [0.70, 11.86]	0.80 [0.30, 2.14]	0.55 [0.20, 1.52]	2.28 [0.57, 9.17]	0.43 [0.15, 1.22]
Age	—	—	1.01 [0.98, 1.04]	1.00 [0.96, 1.03]	1.02 [0.99, 1.05]	1.01 [0.97, 1.04]	1.00 [0.96, 1.03]	1.00 [0.97, 1.03]
cN (7th ed)								
cN0	—	—	1	1	1	—	—	—
cN+	—	—	3.27** [1.34, 8.00]	0.90 [0.26, 3.15]	2.46 [0.93, 6.51]	—	—	—
Surgical margins								
Negative	—	—	—	—	—	1	1	1
Positive	—	—	—	—	—	18.37** [4.19, 80.60]	2.61 [0.46, 14.85]	33.03** [6.87, 158.76]
Neck dissection								
c/pN0	—	—	—	—	—	1	1	1
pN+ ECE−	—	—	—	—	—	2.97 [0.71, 12.33]	2.22 [0.28, 17.65]	2.25 [0.52, 9.78]
pN+ ECE+	—	—	—	—	—	14.51** [3.62, 58.18]	1.82 [0.27, 12.17]	14.77** [3.52, 62.00]
Radiomic score	16.93** [6.28, 45.66]	18.88** [3.12, 114.03]	—	24.49** [7.00, 85.71]	15.84** [2.29, 109.54]	—	24.11** [7.12, 81.61]	40.30** [5.74, 282.99]
C-index	0.98 [0.98, 1.00]	0.68 [0.65, 0.91]	0.68 [0.48, 0.71]	0.98 [0.98, 1.00]	0.73 [0.66, 0.89]	0.77 [0.67, 0.85]	0.98 [0.98, 1.00]	0.83 [0.89, 1.00]
LRT test	—	—	—	<0.001**	0.005**	—	<0.001**	<0.001**

*For $p < 0.05$; **For $p < 0.01$.

TABLE 3 Cause specific mortality regression table for ADC and CE-T1 sequences.

	Pre-treatment model					Post-treatment model		
	Radiomic		Clinical	Clinical radiomic		Clinical	Clinical radiomic	
Sequence Variables	ADC HR [95%CI]	CE-T1 HR [95%CI]	 HR [95%CI]	ADC HR [95%CI]	CE-T1 HR [95%CI]	 HR [95%CI]	ADC HR [95%CI]	CE-T1 HR [95%CI]
Sex								
F	—	—	1	1	1	1	1	1
M	—	—	0.47 [0.19, 1.13]	0.67 [0.25, 1.77]	0.53 [0.21, 1.36]	0.36* [0.15, 0.88]	0.58 [0.22, 1.51]	0.49 [0.20, 1.22]
Age	—	—	1.02 [0.99, 1.05]	1.02 [0.99, 1.05]	1.02 [1.00, 1.06]	1.02 [0.99, 1.05]	1.02 [0.99, 1.06]	1.03 [1.00, 1.06]
Stage (7th ed)								
I–II	—	—	1	1	1	—	—	—
III–IV	—	—	3.85* [1.13, 13.15]	0.60 [0.14, 2.65]	0.87 [0.22, 3.52]	—	—	—
Neck dissection								
c/pN0	—	—	—	—	—	1	1	1
pN+ ECE−	—	—	—	—	—	12.33** [2.56, 59.47]	3.76 [0.72, 19.57]	3.17 [0.56, 17.78]
pN+ ECE+	—	—	—	—	—	12.87** [2.84, 58.38]	5.08* [1.07, 24.21]	5.73* [1.20, 27.25]
Radiomic score	5.28** [3.03, 9.20]	6.29** [3.43, 11.55]	—	6.00** [3.06, 11.74]	6.65 ** [3.37, 13.12]	—	4.37** [2.28, 8.37]	5.53** [2.63, 11.64]
C-index	0.85 [0.77, 0.91]	0.84 [0.76, 0.90]	0.66 [0.59, 0.80]	0.85 [0.75, 0.90]	0.85 [0.73, 0.86]	0.77 [0.70, 0.86]	0.86 [0.79, 0.91]	0.87 [0.79, 0.91]
LRT test	—	—	—	<0.001**	<0.001**	—	<0.001**	<0.001**

*For $p < 0.05$; **For $p < 0.01$.

TABLE 4 Overall survival regression table for ADC and CE-T1 sequences.

	Pre-treatment model					Post-treatment model		
	Radiomic		Clinical	Clinical radiomic		Clinical	Clinical radiomic	
Sequence	ADC	CE-T1		ADC	CE-T1		ADC	CE-T1
Variable	HR [95%CI]	HR [95%CI]	HR [95%CI]	HR [95%CI]	HR [95%CI]	HR [95%CI]	HR [95%CI]	HR [95%CI]
Sex								
F	—	—	1	1	1	1	1	1
M	—	—	0.46* [0.22, 0.96]	0.39* [0.19, 0.82]	0.59 [0.28, 1.27]	0.31* [0.15, 0.67]	0.31** [0.14, 0.65]	0.47* [0.22, 0.99]
Age	—	—	1.02 [1.00, 1.04]	1.02 [1.00, 1.04]	1.04** [1.01, 1.07]	1.03* [1.00, 1.06]	1.03* [1.01, 1.06]	1.05** [1.02, 1.08]
Stage (7th ed)								
I–II	—	—	1	1	1	—	—	—
III–IV	—	—	2.72* [1.04, 7.11]	1.08 [0.35, 3.28]	0.98 [0.31, 3.08]	—	—	—
Neck dissection								
c/pN0	—	—	—	—	—	1	1	1
pN+ ECE−	—	—	—	—	—	7.28** [2.05, 25.88]	4.58* [1.20, 17.42]	2.89 [0.74, 11.34]
pN+ ECE+	—	—	—	—	—	14.78** [4.67, 46.81]	10.21** [2.94, 35.43]	7.07** [2.03, 24.63]
Radiomic score	19.70** [5.57, 69.59]	5.92** [3.32, 10.56]	—	22.17** [4.83, 101.81]	8.15** [3.89, 17.09]	—	7.72** [1.83, 32.49]	6.40** [2.81, 14.55]
C-index	0.72 [0.59, 0.78]	0.79 [0.69,0.84]	0.70 [0.57, 0.77]	0.76 [0.62, 0.78]	0.82 [0.73,0.86]	0.82 [0.74, 0.86]	0.84 [0.79, 0.92]	0.86 [0.80, 0.91]
LRT test	—	—	—	<0.001**	<0.001**	—	0.005**	<0.001**

*For $p < 0.05$; **For $p < 0.01$.

improved, and the stage was no more significant. For LRR pN+ ECE+ versus c/pN0 resulted to be the only significant variable associated with a higher risk of recurrence for OTSCC, as already reported in previous studies.[13,17,20,25] For CSM only Stage III–IV versus I–II was significantly associated with a worse outcome. After adding the radiomic score in LRR and CSM in multivariate analysis only the radiomic score was significant with a C-index improvement. The lack of significance of stage and pN+ ECE+ at multivariable analysis including radiomic score suggests that radiomic features may incorporate information related to stage and to advanced disease, thus becoming the main outcomes predictor. For ADC, Stages III–IV have a significantly higher radiomic score, and pN+ ECE– have a significantly lower radiomic score value with analogous results for CE-T1, DWI and T2W sequences. The combination of clinical variables routinely collected with radiomic features quantitatively extracted from pre-treatment MRI, can increase predictive accuracy for recurrence and mortality prediction. Radiomics models result independent factors in prognosis prediction, regardless of standard clinical factors and treatment.

To the best of our knowledge, this is the first study of radiomics for OTSCC that includes multiple MRI sequences and survival outcomes as clinical endpoints. At the current time only four studies focused on MRI-based radiomics in oral cavity cancer and only one focused on survival outcomes.[26]

Frood et al.[27] (2018) conducted a retrospective study on 115 cases of oral cavity SCC to detect MRI radiomic textures indicative of lymphadenopathy with ENE. Nodal entropy derived from CE-T1 was significant in predicting ENE and nodal entropy combined with irregular boundary was the best predictor of ENE.

Ren et al.[28] (2020) applied radiomics on ADC MRI map of 88 patients with OTSCC distinguishing the degree of differentiation. Also Yu et al.[29] (2021) conduced an analysis on 127 OTSCC determining the degree of differentiation through radiomics on MRI fat-suppressed T2W images. Wang et al.[26] (2021) conducted a retrospective study on 236 patients with tongue cancer. MRI based radiomics of primary tumor and peritumoral tissue resulted an independent indicator for poor disease-free survival and overall survival.

A review published by Jethanandani et al.[6] in 2018 stated that MRI-based radiomics in head and neck district is currently a "young" and unexplored field for several reasons: anatomical complexity of head and neck region, lack of a common ontology, insufficient data source, impact of different scanners, acquisition parameters and image analysis methodologies are potential sources of bias. Furthermore, the multiparametric MRI analysis introduces the challenges related to each sequence, which can exhibit different properties (spatial resolution, signal/noise ratio, possible signal anisotropy).[30] We are aware of the limitations of our study, mainly including suboptimal subject numbers, lack of internal and external validation. In this study, we adopted methodological choices aimed at maximizing the robustness of the extracted features. We tried to overcome the problem of image variability through rigorous MRI selection: all exams were acquired on the same scanner with fixed acquisition parameters (TE, TR, voxel size). We calculated radiomic features from different image types (wavelet, Laplacian of Gaussian, squared, square root, logarithm, exponential, gradient, local binary pattern maps), identifying the procedure that maximizes the ability to predict clinical endpoints. We performed in-sample cross validation to validate our statistical models. Furthermore, the relatively small sample size avoided performing an external validation of our models, rising a possible overfitting. We performed several analyses to address this point, including 5-cross-validation of the parameter λ, bootstrap resampling to obtain the 95%CI and finally an in-sample 5-fold-cross-validation with calculation of average C-index on the test sets, providing similar results (Supplementary Table S5). Our analysis underlined that MRI-based radiomics in clinical practice provides important pre-treatment information in OTSCC contributing to the creation of highly individualized algorithms for treatment and follow-up. Future developments of this project will be founded validation in a multicentric study.

5 | CONCLUSIONS

In conclusion, radiomics application to preoperative MRI of patients with OTSCC represents a promising and noninvasive method of precision medicine. The integration of radiomics to standard clinical models has the potential to increase the accuracy in estimating the prognosis of these patients, providing accurate information before surgery. Furthermore, our results show that radiomics models are independent factors in prognosis prediction, regardless of standard clinical factors and type of surgery treatment. The incorporation of radiomics into clinical practice will likely contribute to improving precision medicine in patients with OTSCC in the future. To achieve these objectives, external validation of our data and other prospective studies of adequate numbers will be needed in the future.

AUTHOR CONTRIBUTIONS

All persons designated as authors participated sufficiently in the work to take public responsibility for the content

of the manuscript: conception, design, analysis and interpretation of data, draft of the manuscript, revision for important intellectual content and final approval of the version to be published.

CONFLICT OF INTEREST STATEMENT

The authors declare no conflicts of interest. The institution of some authors (European Institute of Oncology) was partially supported by the Italian Ministry of Health with Progetto di Eccellenza, Ricerca Corrente and 5x1000 funds. Stefania Volpe MD and Lars Johannes Isaksson MSc are PhD students within the European School of Molecular Medicine (SEMM), Milan.

ACKNOWLEDGMENT

Open access funding provided by BIBLIOSAN.

DATA AVAILABILITY STATEMENT

The data that support the findings of this study are available from the corresponding author upon reasonable request.

ORCID

Marta Tagliabue https://orcid.org/0000-0002-7879-4846
Stefania Volpe https://orcid.org/0000-0003-0498-2964
Giulia Marvaso https://orcid.org/0000-0002-5339-8038
Mohssen Ansarin https://orcid.org/0000-0002-8384-5388

REFERENCES

1. Keek SA, Leijenaar RT, Jochems A, Woodruff HC. A review on radiomics and the future of theranostics for patient selection in precision medicine. *Br J Radiol*. 2018;91(1091):20170926. doi:10.1259/bjr.20170926
2. Aerts HJ. The potential of radiomic-based phenotyping in precision medicine: a review. *JAMA Oncol*. 2016;2(12):1636-1642. doi:10.1001/jamaoncol.2016.2631
3. Aerts HJ, Velazquez ER, Leijenaar RT, et al. Decoding tumour phenotype by noninvasive imaging using a quantitative radiomics approach. *Nat Commun*. 2014;5:4644. doi:10.1038/ncomms5006
4. Song J, Yin Y, Wang H, Chang Z, Liu Z, Cui L. A review of original articles published in the emerging field of radiomics. *Eur J Radiol*. 2020;127:108991. doi:10.1016/j.ejrad.2020.108991
5. Peng Z, Wang Y, Wang Y, et al. Application of radiomics and machine learning in head and neck cancers. *Int J Biol Sci*. 2021;17(2):475-486. doi:10.7150/ijbs.55716
6. Jethanandani A, Lin TA, Volpe S, et al. Exploring applications of radiomics in magnetic resonance imaging of head and neck cancer: a systematic review. *Front Oncol*. 2018;14(8):131. doi:10.3389/fonc.2018.00131
7. Mahajan A, Ahuja A, Sable N, Stambuk HE. Imaging in oral cancers: a comprehensive review. *Oral Oncol*. 2020;104:104658. doi:10.1016/j.oraloncology.2020.104658
8. Moreira MA, Lessa LS, Bortoli FR, et al. Meta-analysis of magnetic resonance imaging accuracy for diagnosis of oral cancer. *PLoS One*. 2017;12(5):e0177462. doi:10.1371/journal.pone.0177462
9. National Comprehensive Cancer Network. *Head and Neck Cancers* (version 02.2022). Accessed June 11, 2022. http://www.nccn.org/professionals/physician_gls/pdf/head-and-neck.pdf
10. Cohen EEW, Bell RB, Bifulco CB, et al. The Society for Immunotherapy of Cancer consensus statement on immunotherapy for the treatment of squamous cell carcinoma of the head and neck (HNSCC). *J Immunother Cancer*. 2019;7(1):184. doi:10.1186/s40425-019-0662-5
11. Bello IO, Soini Y, Salo T. Prognostic evaluation of oral tongue cancer: means, markers and perspectives (I). *Oral Oncol*. 2010;46(9):630-635. doi:10.1016/j.oraloncology.2010.06.006
12. Brenner H. Long-term survival rates of cancer patients achieved by the end of the 20th century: a period analysis. *Lancet*. 2002;360(9340):1131-1135. doi:10.1016/S0140-6736(02)11199-8
13. Zanoni DK, Montero PH, Migliacci JC, et al. Survival outcomes after treatment of cancer of the oral cavity (1985–2015). *Oral Oncol*. 2019;90:115-121. doi:10.1016/j.oraloncology.2019.02.001
14. Lenze NR, Farquhar DR, Dorismond C, et al. Age and risk of recurrence in oral tongue squamous cell carcinoma: systematic review. *Head Neck*. 2020;42(12):3755-3768. doi:10.1002/hed.26464
15. Faisal M, Dhanani R, Ullah S, et al. Prognostic outcomes of treatment naïve oral tongue squamous cell carcinoma (OTSCC): a comprehensive analysis of 14 years. *Eur Arch Otorhinolaryngol*. 2021;278(8):3045-3053. doi:10.1007/s00405-020-06482-x
16. Oliver JR, Wu SP, Chang CM, et al. Survival of oral tongue squamous cell carcinoma in young adults. *Head Neck*. 2019;41(9):2960-2968. doi:10.1002/hed.25772
17. Cooper JS, Pajak TF, Forastiere AA, et al. Radiation Therapy Oncology Group 9501/Intergroup. Postoperative concurrent radiotherapy and chemotherapy for high-risk squamous-cell carcinoma of the head and neck. *N Engl J Med*. 2004;350(19):1937-1944. doi:10.1056/NEJMoa032646
18. Tam S, Amit M, Zafereo M, Bell D, Weber RS. Depth of invasion as a predictor of nodal disease and survival in patients with oral tongue squamous cell carcinoma. *Head Neck*. 2019;41(1):177-184. doi:10.1002/hed.25506
19. Mannelli G, Comini LV, Piazza C. Surgical margins in oral squamous cell cancer: intraoperative evaluation and prognostic impact. *Curr Opin Otolaryngol Head Neck Surg*. 2019;27(2):98-103. doi:10.1097/MOO.0000000000000516
20. Ganly I, Patel S, Shah J. Early stage squamous cell cancer of the oral tongue—clinicopathologic features affecting outcome. *Cancer*. 2012;118(1):101-111. doi:10.1002/cncr.26229
21. Zumsteg ZS, Luu M, Kim S, et al. Quantitative lymph node burden as a 'very-high-risk' factor identifying head and neck cancer patients benefiting from postoperative chemoradiation. *Ann Oncol*. 2019;30(1):76-84. doi:10.1093/annonc/mdy490
22. Ansarin M, Bruschini R, Navach V, et al. Classification of GLOSSECTOMIES: proposal for tongue cancer resections. *Head Neck*. 2019;41(3):821-827. doi:10.1002/hed.25466

23. Tagliabue M, Gandini S, Maffini F, et al. The role of the T-N tract in advanced stage tongue cancer. *Head Neck*. 2019;41(8):2756-2767. doi:10.1002/hed.25761
24. Thoeny HC, De Keyzer F, King AD. Diffusion-weighted MR imaging in the head and neck. *Radiology*. 2012;263(1):19-32. doi:10.1148/radiol.11101821
25. García J, López M, López L, et al. Validation of the pathological classification of lymph node metastasis for head and neck tumors according to the 8th edition of the TNM classification of malignant tumors. *Oral Oncol*. 2017;70:29-33. doi:10.1016/j.oraloncology.2017.05.003
26. Wang F, Tan R, Feng K, et al. Magnetic resonance imaging-based radiomics features associated with depth of invasion predicted lymph node metastasis and prognosis in tongue cancer. *J Magn Reson Imaging*. 2021;56:196-209. doi:10.1002/jmri.28019
27. Frood R, Palkhi E, Barnfield M, Prestwich R, Vaidyanathan S, Scarsbrook A. Can MR textural analysis improve the prediction of extracapsular nodal spread in patients with oral cavity cancer? *Eur Radiol*. 2018;28(12):5010-5018. doi:10.1007/s00330-018-5524-x
28. Ren J, Qi M, Yuan Y, Tao X. Radiomics of apparent diffusion coefficient maps to predict histologic grade in squamous cell carcinoma of the oral tongue and floor of mouth: a preliminary study. *Acta Radiol*. 2021;62(4):453-461. doi:10.1177/0284185120931683
29. Yu B, Huang C, Xu J, et al. Prediction of the degree of pathological differentiation in tongue squamous cell carcinoma based on radiomics analysis of magnetic resonance images. *BMC Oral Health*. 2021;21(1):585. doi:10.1186/s12903-021-01947-9
30. Li R, Li L, Xu Y, Yang J. Machine learning meets omics: applications and perspectives. *Brief Bioinform*. 2021;23(1):bbab460. doi:10.1093/bib/bbab460

SUPPORTING INFORMATION

Additional supporting information can be found online in the Supporting Information section at the end of this article.

How to cite this article: Mossinelli C, Tagliabue M, Ruju F, et al. The role of radiomics in tongue cancer: A new tool for prognosis prediction. *Head & Neck*. 2023;45(4):849-861. doi:10.1002/hed.27299